Separation & Purification Reviews
Publication details, including instructions for authors and subscription information:
http://www.informaworld.com/smpp/title~content=t713597294

Analysis of the Apollo 16 Free-Fluid Electrophoresis Experiment

F. J. Micale[a]; J. W. Vanderhoff[a]; R. S. Snyder[b]
[a] Center for Surface and Coatings Research Lehigh University Bethlehem, Pennsylvania [b] National Aeronautics and Space Administration George C. Marshall Space Flight Center Huntsville, Alabama

To cite this Article Micale, F. J. , Vanderhoff, J. W. and Snyder, R. S.(1976) 'Analysis of the Apollo 16 Free-Fluid Electrophoresis Experiment', Separation & Purification Reviews, 5: 2, 361 — 383

To link to this Article: DOI: 10.1080/03602547608069360

URL: http://dx.doi.org/10.1080/03602547608069360

SEPARATION AND PURIFICATION METHODS, 5(2), 361-383 (1976)

ANALYSIS OF THE APOLLO 16 FREE-FLUID ELECTROPHORESIS EXPERIMENT

F. J. Micale and J. W. Vanderhoff
Center for Surface and Coatings Research
Lehigh University
Bethlehem, Pennsylvania 18015

R. S. Snyder
National Aeronautics and Space Administration
George C. Marshall Space Flight Center
Huntsville, Alabama 35812

ABSTRACT

The Apollo 16 free-fluid electrophoresis experiment attempted the separation in microgravity of two different-size monodisperse polystyrene latexes under conditions that would give a completely roiled sample on earth because of the thermal convection. The instrument comprised three parallel 0.63-cm inside diameter 10.2-cm long Lexan polycarbonate electrophoresis channels, with the electrodes separated from the channel by semipermeable membranes. The latex samples were contained in cylindrical chambers separated from the electrode by a fixed semipermeable membrane and from the Lexan tube by a movable Kapton polyimide film. Two channels contained 0.80μm- and 0.23μm-diameter monodisperse polystyrene latexes and the third, a mixture of the two sizes. The experiment was initiated in microgravity by removing the Kapton films which separated the latex samples from the electrophoresis channels and applying a potential of 300 volts across the electrodes. The results were recorded by photographs taken every 20 seconds.

In all three channels, the latex particle profiles were elongated, bullet-shaped parabolas, and there was no indication of separation of the particle mixture. This paper describes the analysis of these results using color contour densitometric analysis of the photographs and ground-based measurements of the electrophoretic mobilities of the particles, the electroosmotic velocity along the channel wall, and the actual potential gradient. This analysis showed that the movement of the particles could be predicted theoretically and that the mixture was indeed separated in the form of two nested parabolic cones. The primary conclusion from these results is that electrophoretic separation is greatly simplified in microgravity because of the absence of thermal convection in the presence of high potential fields.

INTRODUCTION

The electrokinetic behavior of biological materials has long been an active and productive area of research. As early as 1860, Kuhne and Jurgenson, in separate publications, described the electrokinetic properties of muscle tissue and biological cells (1). Since that time, biologists have shown that the electrical double-layer properties of the cell wall/liquid interface often reflect the biological characteristics of the cells. Therefore, electrophoresis is potentially a powerful tool for separating biological cells according to their biological properties.

There are many problems that must be solved to develop a practical method for electrophoretic separation of biological cells. In principle, however, two major problems could be alleviated by carrying out the separation in space. The first and more serious problem is thermal convection, which is brought about by the joule heating resulting from the electric current in the liquid medium. The second problem is the settling of large biological cells of density greater than that of the medium. Both of these problems would be eliminated by carrying out the electrophoretic separation in the microgravity environment of an earth orbit vehicle. The other problems of electrophoretic separation are of an experimental nature and involve primarily the design of the electrophoresis cell to give maximum resolution of separation combined with the capability of efficient collection of the separated fractions.

To take advantage of the benefits of microgravity, NASA initiated an experimental program on electrophoretic separation as part of its space processing program. The first electrophoretic separation in microgravity was performed on the Apollo 14 mission* on the return trip from the moon, when a mixture of red and blue dyes was separated with sharper boundaries than could be achieved in comparable experiments on earth (2). The next experiment on Apollo 16* used the basic components of the Apollo 14 electrophoretic separation instrument for the separation of model colloid particles, to serve as a prelude to the later separation of viable biological cells. The model particles selected were monodisperse polystyrene latex particles of different size (and, hence, different electrophoretic mobility). The experiment was performed on the day after the launch of Apollo 16 by Astronaut T. K. Mattingly, who made photographs and observations of the separation.

The experiment comprised the electrophoresis of three latex samples --- 0.80μm- and 0.23μm-diameter particles separately and a mixture of the two sizes --- in parallel cylindrical channels. It was hoped that the mixture of the two different particle sizes would separate into discrete bands. Instead, the particle profiles were those of an elongated bullet-shaped parabola (see Figure 1), which obscured any separation of the two sizes. The analysis of the experiment, however, showed that separation had indeed occurred as expected, but was obscured

---

* Instrument developed and constructed by General Electric Company, Valley Forge, Pa. 19481.

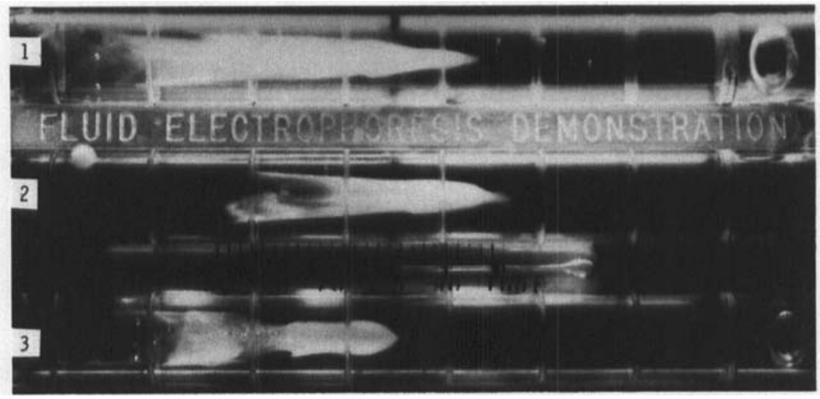

FIGURE 1

Apollo 16 Electrophoresis (Frame 17013) after 200 seconds

by the strong electroosmotic flow of the liquid medium along the channel wall in a direction opposite to that of the electrophoresis. The details of the experimental apparatus, the photographs and observations made during the course of the experiment, and the conclusions drawn from the experimental analysis were reported earlier (3). The purpose of this paper is to describe in detail the analysis of the experimental results that led to the conclusion that separation of the two different particle sizes had indeed occurred.

EXPERIMENTAL DETAILS AND RESULTS OF THE APOLLO 16 EXPERIMENT

The experimental details and results were described earlier (3) and will be reviewed only briefly here. The Apollo 16 electrophoresis instrument comprised three parallel 0.63-cm inside diameter 10.2-cm long Lexan polycarbonate tubes separated from the electrode compartments by semipermeable membranes. Thus the electrophoresis was carried out in a closed system and therefore was the free-fluid type. The two monodisperse latex polystyrene latexes selected were Lots LS-1200-B (0.80μm diameter) and LS-1047-E (0.23μm diameter) (4). The dispersion medium was an aqueous solution containing 0.008M boric acid and 0.0016M sodium hydroxide as buffer, 0.00069M sodium lauryl sulfate emulsifier, and 0.033M formalin perservative. Prior to the start of the experiment, the latex samples were isolated in a 0.48 cm-diameter cylindrical chamber, separated from the cathode by a fixed semi-permeable membrane and from the Lexan tube by a removable Kapton polyimide film. To start the experiment, the Kapton film was removed so that the latex particles were free to migrate into the Lexan tube, and a potential of 300 volts was applied across·platinum electrodes 11.5 cm apart.

The progress of the electrophoresis was followed by photographs taken automatically every 20 seconds. As soon as the particles were released to the Lexan tube and the voltage gradient applied, they began to migrate rapidly, forming elongated bullet-shaped parabolic profiles. Figure 1 shows the electrophoretic separation at 200 seconds after initiation of the experiment; Tube 1 contained the mixture of the two different sizes, Tube 2 the 0.80μm-diameter particles, and Tube 3 the 0.23μm-diameter particles. It can be seen that the temperature inside the instrument case was 81° F, increasing from the initial 76° F during the 200-second period (the temperature rise inside the Lexan tubes was probably even greater). The electrophoretic separation was continued for a total time of 280 seconds at which time the faster-moving 0.80μm-diameter particles approached the end of the channel. The current was then reversed, so that the direction of travel of the particles was reversed. Altogether, 52 photographs were taken of four traversals of the channel by the latex particles; however, the most useful information for analysis of the experiment was in the 14 frames depicting the first traversal.

These elongated particle profiles, which are the result of a strong electroosmotic flow of the liquid medium backwards along the channel wall, completely obscured any separation of the different-size particles in Tube 1. Although this elongated profile could be the result of combining the profiles of Tubes 2 and 3 to form two nested parabolic cones, there was no visual evidence that separation of the two different-size particles had occurred.

THEORETICAL ASPECTS OF FREE-FLUID ELECTROPHORESIS

The observed velocity V_{obs} of a colloidal particle subjected to an applied potential in a closed cylindrical channel is defined by the equation:

$$V_{obs} = V_e + V \tag{1}$$

where V_e is the velocity of the particle due to electrophoresis, and V is the solvent velocity due to electroosmosis. The solvent velocity V under these conditions is defined by the equation:

$$V = U\,[(2r^2/a^2) - 1], \tag{2}$$

where r is the distance from center of channel, a the radius of channel, and U the electroosmotic velocity of solvent at the channel wall (i. e., where $r = a$). Combining Equations 1 and 2 yields:

$$V_{obs} = V_e + U\,[(2r^2/a^2) - 1]\ . \tag{3}$$

Equation 3 predicts that the observed particle velocity is a sensitive function of r and is described by a parabola that is symmetric about the center of the channel. Since information obtained from the Apollo 16 experiment was in the form of photographs taken every 20 seconds, the position that could be followed and measured accurately was the apex of the parabola at the center of the channel, i. e., at $r = 0$. At $r = 0$, Equation 3 reduces to:

$$V_{obs} = V_e - U . \qquad (4)$$

A potential of 300 volts applied to a cell of these dimensions gives a potential gradient of 26 volts/cm. However, there are "a posteriori" reasons for suspecting the constancy and absolute value of this potential gradient during the course of the experiment.

The potential gradient may be separated from the right hand side of Equation 4 as follows:

$$V_{obs} = (U_e - U_{os}) E \qquad (5)$$

where $\underline{U}_e$ is the electrophoretic mobility of the particle, $\underline{U}_{os}$ the electro-osmotic mobility of the solvent, and $\underline{E}$ the potential gradient. The particle velocity in the center of the channel, therefore, is a function of the electrophoretic mobility of the particles, the electroosmotic mobility of the medium at the channel wall, and the applied potential gradient.

EXPERIMENTAL DETAILS AND RESULTS OF GROUND-BASED EXPERIMENTS

Electrophoretic Mobility of Polystyrene Latex Particles by Microcapillary Electrophoresis

The electrophoretic mobilities of the 0.80μm- and 0.23μm-diameter monodisperse polystyrene latex particles were measured in a microcapillary electrophoresis apparatus (Rank Brothers, Ltd.) at an applied potential of 1.7 volts/cm. This 2mm-diameter cylindrical microcapillary cell had a wall thickness less than 0.1mm, thus giving distortionless viewing at all levels without the necessity for optical corrections. The zero-solvent-flow level in this cell was defined accurately by measuring the parabolic particle velocity profile across the diameter of the cell for particles of different electrophoretic mobilities. The conventional light source used with this instrument was a quartz-iodine lamp in the dark-field configuration. This light source was adequate to detect the 0.80μm-diameter particles, but not the 0.23μm-diameter particles. Therefore, a 5 mv He-Ne laser (Model ML411, Metrologic Instruments, Inc.) was used as the light source, with remarkable success in detecting the 0.23μm-diameter particles.

The dispersion mediums used were various modifications of the borate buffer medium used in the Apollo 16 experiment. The average electrophoretic mobilities in the standard buffer medium used in the Apollo 16 experiment were 9.2 and 6.5 μm cm/volt sec for the 0.80μm- and 0.23μm-diameter particles, respectively. There was no detectable change in electrophoretic mobility of these particles after storage in this medium for two weeks.

Potential Gradient in the Apollo 16 Electrophoresis Channels

An important parameter in analyzing the results of the Apollo 16 electrophoresis experiment is the actual value of the potential gradient $\underline{E}$ in each electrophoresis channel. The potential of 300 volts applied across the 11.5-cm distance between the electrodes gives a calculated potential gradient of 26 volts/cm. Approximate calculations of the rate of travel of the particles, however, suggested that the actual values were significantly less than the calculated value. Two factors that could reduce the value to $\underline{E}$ below the calculated value are the semipermeable membranes that were used to close both ends of the electrophoresis channel and the bubbles which appeared both inside and outside the channels (see those in Tubes 1 and 3 of Figure 1).

Therefore, an attempt was made to measure the potential gradient within the channel by ground-based experiments. Figure 2 shows a schematic representation of the electrophoresis instrument constructed to

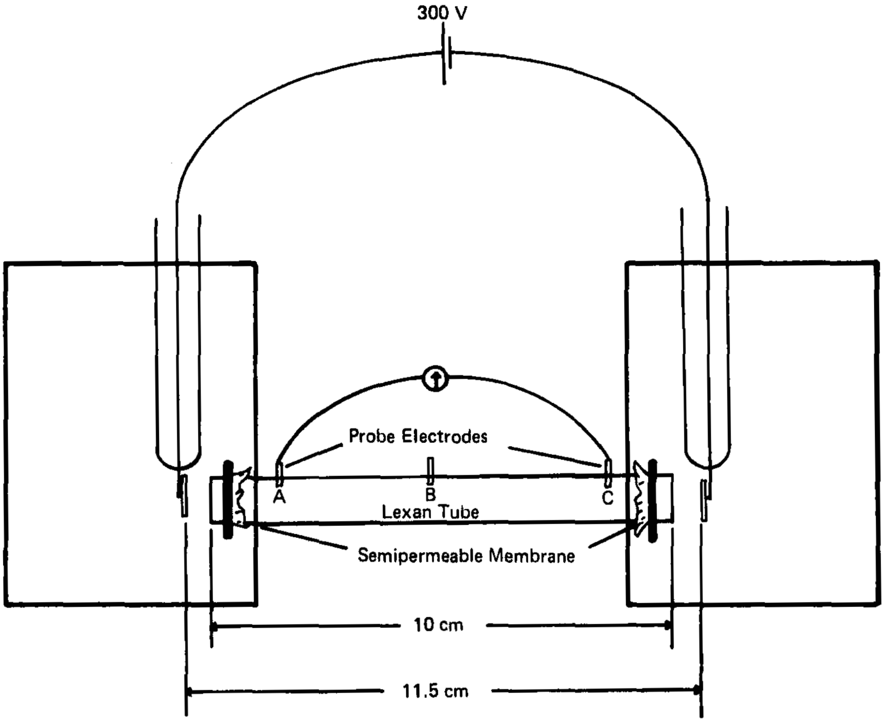

FIGURE 2

Schematic Representation of Electrophoresis Channel for Measuring Potential Gradient E

make these measurements. The main features of this instrument were identical to that used in the Apollo 16 experiment. The Lexan tube was of the same dimensions and the semipermeable membranes were of the same material. The three probe electrodes A, B, and C were used to measure the potential gradient at different positions in the Lexan tube when a potential of 300 volts was applied across the main electrodes.

The measurements made with this instrument with no bubbles in the channel showed that the semipermeable membranes used in the Apollo 16 experiment had no effect on the potential gradient. When bubbles were introduced into the channel, the potential gradient was decreased by as much as 5%, depending upon the size of the bubble. When the bubble was placed at the end of the channel in contact with the semipermeable membrane, the potential gradient was decreased by as much as 10%. These values may not be valid, however, because of the tendency of the bubbles to rise and flatten against the top of the channel, thus offering less resistance on earth than in microgravity where their shape would be spherical.

Therefore, 5-mm glass beads were placed in the channel to approximate more closely the air bubbles in the Apollo 16 experiment. These spherical glass beads had a much greater effect in decreasing the potential gradient within the channel. The decrease in $\underline{E}$ ($\Delta \underline{E}$) was inversely proportional to the cross-sectional area of the channel minus the cross-sectional area of the glass bead according to the equation:

$$\Delta E = K/(d_1^2 - d_2^2) \qquad (6)$$

where $\underline{K}$ is a constant, $\underline{d}_1$ the diameter of the channel, and $\underline{d}_2$ the diameter of the glass bead (or air bubble, assuming the resistances to be about the same for these purposes). Since $\Delta \underline{E}$ was found to be 2.5 volts/cm for $\underline{d}_2 = 0.5$ cm, $\underline{K} = 0.4$.

The photographic record of the Apollo 16 experiment showed that the bubble diameters were 0.6 cm or greater. Equation 6 predicts that the value of $\Delta \underline{E}$ is 10 volts/cm when the bubble diameter is 0.60 cm and 15 volts/cm when the bubble diameter is 0.61 cm. Apparently, $\underline{E}$ decreases rapidly as the bubble diameter approaches the inside diameter of the channel. Experimental tests with beads larger than 0.5 cm in diameter were not possible because the geometric tolerances of these glass beads were about 25%, with the result that the larger beads would not fit into the channel. Nevertheless, the foregoing theory and experimental results suggest that the air bubbles present in the Apollo 16 electrophoresis channels drastically reduced the potential gradient within the channels.

Electroosmosis in the Apollo 16 Electrophoresis Channels

The electroosmotic flow at the Lexan channel wall/buffer solution interface was measured by placing the electrophoresis instrument shown in Figure 2 on the stage of a microscope and observing the particle velocities at 250X magnification. The optical properties of the Lexan tube were improved by polishing the top surface to a flat configuration. Even so, some difficulty was encountered in observing particles at different depths in the channel.

Monodisperse polyvinyltoluene particles of 2.02μm diameter (4) with an average electrophoretic mobility of 10μm cm/volt sec in the standard buffer medium as measured by microcapillary electrophoresis were used to measure the velocity of the medium next to the channel wall. When the velocity of these particles was measured as a function of depth in the channel, it was found that they changed direction near the channel wall, indicating that the electroosmotic velocity at the Lexan/buffer solution interface was greater than -10μm cm/volt sec. The negative sign is used to indicate that the buffer medium moves toward the cathode as opposed to the negatively-charged polyvinyltoluene particles, which move toward the anode. Thus these experiments show that the electroosmotic mobility of the Lexan surface in this buffer medium is greater than the electrophoretic mobilities of the polystyrene particles to be separated.

ANALYSIS OF RESULTS OF THE APOLLO 16 ELECTROPHORESIS EXPERIMENT

The details of the experimental apparatus and the flight photographs, which were the source of all experimental results were described earlier

(5) and hence are not included here. The photographs, numbered sequentially beginning with Frame 17001, were taken automatically every 20 seconds. The experiment was initiated (i. e., time = 0) at Frame 17003, and the current was first reversed at Frame 17017 (280 seconds after the start of the experiment) when the fastest-moving particles approached the end of the channel. Although 52 photographs were taken during the four traversals of latex particles, the useful information for analysis was in the first 14 frames after the current was turned on. Figure 2 shows one of the flight photographs (Frame 17013) which was taken 200 seconds after initiation of the experiment.

The initial appearance of the latex particles (Frame 17005, time = 40 seconds) showed that the observed velocity of the latex particles was influenced by electroosmotic flow of the medium as evidenced by the sharp parabolic particle profile. The position of the apex of the parabola as a function of time is shown in Figure 3. Tube 1 contained the mixture of 0.80μm- and 0.23μm-diameter particles, while Tube 2 contained the 0.80μm diameter particles and Tube 3 the 0.23μm diameter particles. The linear variation of position with time for the first three minutes of the experiment shows that the particles were traveling at a constant velocity during this period. Extrapolation of the results to zero time, however, indicates that the latex particles in Tubes 1 and 3 were delayed in the sample chamber for 7 and 9 seconds, respectively. The change in slope beyond three minutes indicates a sudden decrease in the potential gradient of all three tubes. This phenomenon can be explained by the presence of the three large bubbles which were located initially at the center of each tube: when the current was turned on, the bubbles migrated toward the anode and reached the end of the tube three to four minutes later; when the bubbles contacted the semipermeable membrane, the resistance increased, resulting in a decrease in the potential gradient. The observed particle velocities at the center of each tube (i. e., at $\underline{r} = 0$) calculated from the data of Figure 3 are given in Table I.

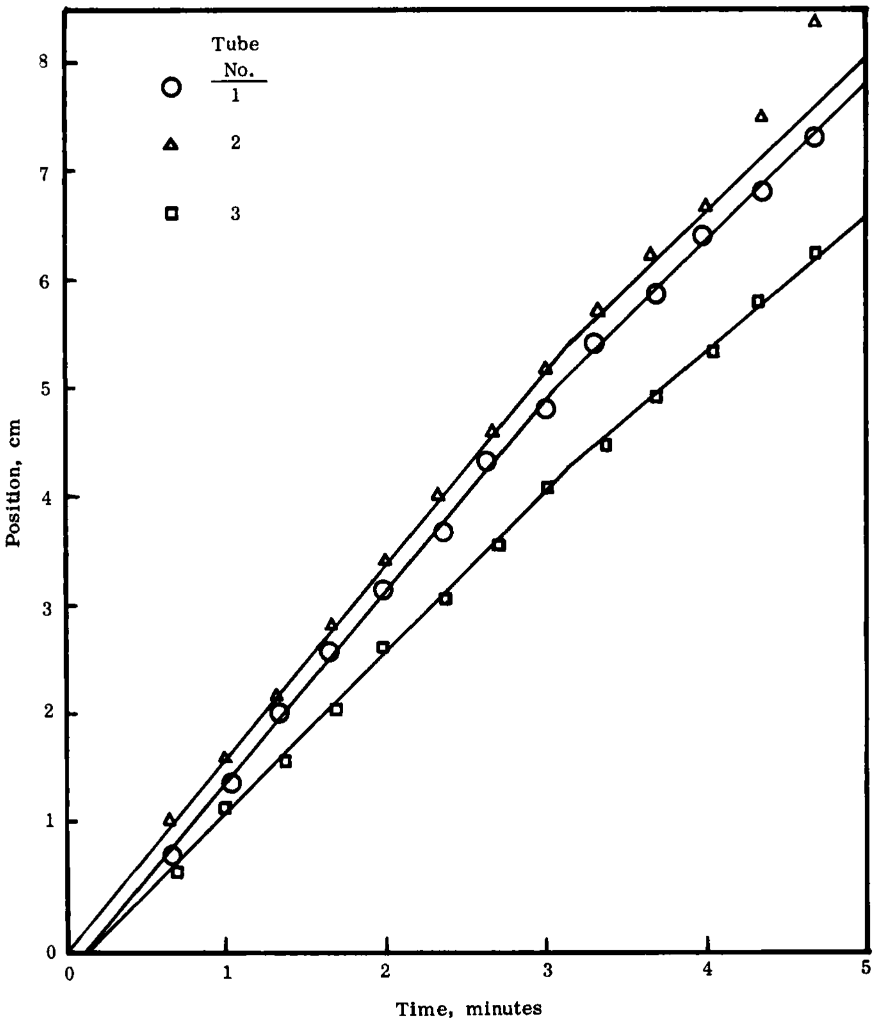

FIGURE 3

Variation of the Position of the Apex of the Parabolic Particle Velocity Profile with Time

An evaluation of the Apollo 16 flight films requires the use of Equation 5 which predicts the observed particle velocity $\underline{V}_{obs}$ in the

TABLE I

Electrophoretic Mobilities and Observed Velocities of Latex Particles*

Tube No.	Latex Particles	Observed Particle Velocity, cm/min Initial	Observed Particle Velocity, cm/min Final	Electrophoretic Mobility,** cm^2/volt min
1	0.23μm + 0.80μm	${}_1V_{obs} = 1.72$	${}_1V'_{obs} = 1.45$	${}_AU_e = 0.0552$
2	0.80μm	${}_2V_{obs} = 1.79$	${}_2V'_{obs} = 1.43$	${}_AU_e = 0.0552$
3	0.23μm	${}_3V_{obs} = 1.49$	${}_3V'_{obs} = 1.26$	${}_BU_e = 0.0392$

* The observed particle velocity V_{obs} is taken at $r = 0$.

** ${}_AU_e$ and ${}_BU_e$ are the electrophoretic mobilities of the 0.80μm- and 0.23μm-diameter latex particles, respectively.

---

center of the channel as a function of the electrophoretic mobility of the latex particles U_e, the electroosmotic mobility at the channel wall/liquid interface U_{os}, and the potential gradient E:

$$V_{obs} = (U_e - U_{os})\,E \qquad (5)$$

Although V_{obs} and U_e are known accurately (Table I), there is some uncertainty in the values of both U_{os} and E. The value of U_{os} was found from laboratory experiments to be at least -10μm cm/volt sec (or -0.06 cm^2/volt min), while E was found to be less than the calculated value of 26 volts/cm. Equation 5 was solved for E_1, E_2, and E_3, the potential gradients in Tubes 1, 2, and 3, respectively, and the following ratios were set up, to estimate which tubes, if any, had identical values of E:

$$\frac{E_2}{E_1} = \frac{{}_2V_{obs}}{{}_1V_{obs}} = 1.04 \tag{7}$$

$$\frac{E_1}{E_3} = \frac{{}_1V_{obs}}{{}_3V_{obs}} \frac{({}_BU_e - U_{os})}{({}_AU_e - U_{os})} = 1.155 \frac{(0.0392 - U_{os})}{(0.0552 - U_{os})} \tag{8}$$

$$\frac{E_2}{E_3} = \frac{{}_2V_{obs}}{{}_3V_{obs}} \frac{({}_BU_e - U_{os})}{({}_AU_e - U_{os})} = 1.200 \frac{(0.0392 - U_{os})}{(0.0552 - U_{os})} \tag{9}$$

When the approximate value of $U_{os} = -0.06$ cm^2/volt min. is substituted into Equations 8 and 9, $E_2/E_1 = 1.04$, $E_1/E_3 = 0.99$, and $E_2/E_3 = 1.03$. These results show clearly that it is reasonable to assume that $E_1 = E_3$. Equation 5 may now be solved for E in tubes 1 and 3:

$$E_1 = \frac{{}_1V_{obs}}{({}_AU_e - U_{os})} \tag{10}$$

$$E_3 = E_1 = \frac{{}_3V_{obs}}{({}_BU_e - U_{os})} \tag{11}$$

Equations 10 and 11 may be equated and rearranged to solve for U_{os}:

$$U_{os} = \frac{{}_3V_{obs}\,{}_AU_e - {}_1V_{obs}\,{}_BU_e}{{}_3V_{obs} - {}_1V_{obs}} \tag{12}$$

Substituting the data in Table I gives $U_{os} = -0.0644$ cm^2/volt min. or -10.7μm cm/volt sec, in good agreement with the experimental approximation presented previously. Using this value of U_{os} and solving Equation 5 for E, the potential gradient may be calculated separately for Tubes 1, 2, and 3 as follows (see Table I for pertinent data):

$$E_1 = \frac{{}_1V_{obs}}{({}_AU_e - U_{os})} = 14.4 \text{ volts/cm} \tag{13a}$$

$$E_2 = \frac{{}_2V_{obs}}{({}_AU_e - U_{os})} = 15.0 \text{ volts/cm} \qquad (13b)$$

$$E_3 = \frac{{}_3V_{obs}}{({}_BU_{os} - U_{os})} = 14.4 \text{ volts/cm} \qquad (13c)$$

The potential gradient beyond 3 minutes, $\underline{E}'$, (past the inflection points of the curves of Figure 3) may be calculated for each tube from the following series of equations (see Table I for pertinent data):

$$E'_1 = \frac{{}_1V'_{obs}}{({}_AU_e - U_{os})} = 12.1 \text{ volts/cm} \qquad (14a)$$

$$E'_2 = \frac{{}_2V'_{obs}}{({}_AU_e - U_{os})} = 12.0 \text{ volts/cm} \qquad (14b)$$

$$E'_3 = \frac{{}_3V'_{obs}}{({}_BU_e - U_{os})} = 12.2 \text{ volts/cm} \qquad (14c)$$

Furthermore, the six Equations 13a-c and 14a-c can be shown to be internally consistent.

Equation 3 may now be expressed in terms of a potential gradient that is not constant for all three tubes:

$$V_{obs} = U_eE + U_{os}E\left\{\frac{2r^2}{a^2} - 1\right\} \qquad (15)$$

Since the values of all the parameters in Equation 15 are known, the particle velocity may be calculated as a function of position $\underline{r}$ in each tube where $\underline{a} = 0.318$ cm. The results for the observed particle velocity $\underline{V}_{obs}$ expressed in cm/min are as follows:

Initial 180 sec of first traverse

$$\text{Tube 1: } {}_1V_{obs} = 1.72 - 18.3\,r^2 \qquad (16a)$$

Tube 2: $_2V_{obs} = 1.79 - 19.1\ r^2$ (16b)

Tube 3: $_3V_{obs} = 1.49 - 18.3\ r^2$ (16c)

Final 100 sec of first traverse

Tube 1: $_1V'_{obs} = 1.45 - 15.4\ r^2$ (17a)

Tube 2: $_2V'_{obs} = 1.43 - 15.3\ r^2$ (17b)

Tube 3: $_3V'_{obs} = 1.26 - 15.5\ r^2$ (17c)

Equations 16 and 17 give the parabolic shape and position of the latex particles in each tube as a function of time. To determine the length of the tail of each parabola, however, requires a knowledge of how close the latex particles approach the channel wall. Since the radius of the sample chamber is smaller than the channel radius, the position of the particles in the channel is a function of the dimensions and solvent flow conditions of the sample chamber, i. e., at some maximum distance from the center of the sample chamber, the particle velocity will be zero so that only the particles at smaller distances may leave the sample chamber. Equation 15 may be used to predict the maximum distance $\underline{r}_{max}$ of the particles measured from the center of the chamber, by setting the observed velocity $\underline{V}_{obs}$ equal to zero and solving for $\underline{r}_{max}$:

$$r_{max} = \frac{a}{\sqrt{2}} \sqrt{\left(1 - \frac{U_e}{U_{os}}\right)} \qquad (18)$$

where the radius of the sample chamber $\underline{a}$ is equal to 0.238 cm. Therefore, Equation 18 predicts that the maximum distances of the latex particles from the center of the channel will be 0.229, 0.229, and 0.214 cm for Tubes 1, 2, and 3, respectively. These results, along with Equations 16 and 17, allow the prediction of the particle profile as a function of time. Figure 4 compares the predicted profiles with the

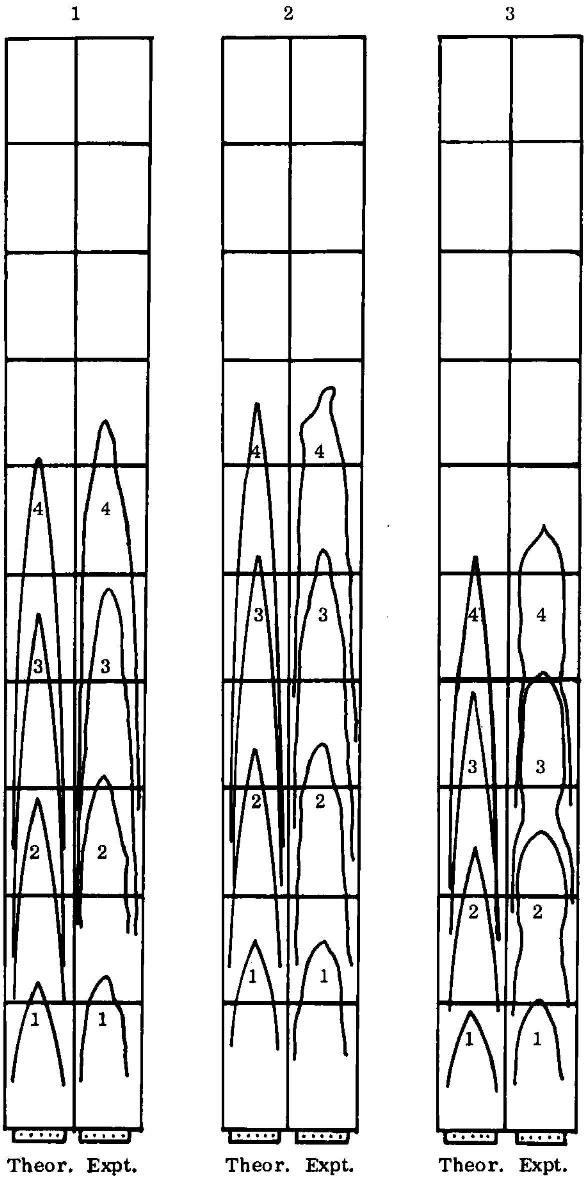

FIGURE 4

Comparison of Theoretical and Calculated Parabolic Particle Profiles at 1, 2, 3, and 4 Minute Intervals results of the Apollo 16 experiment for Tubes 1, 2, and 3 at the indicated times of 1, 2, 3, and 4 minutes. The agreement between experiment and theory is remarkably good; however, the theory cannot explain the irregular particle profile observed in Tube 3.

Another important parameter that can be evaluated from theory and compared with experiment is length of the parabolic particle profile as a function of time. The velocity of parabolic growth may be calculated by subtracting the velocity of the particles at the tail of the parabola (i.e., at $\underline{r} = \underline{r}_{max}$) from the velocity of the particles at the apex of the parabola (i.e., at $\underline{r} = 0$). For the case of Tube 1, Equation 16a is used to calculate particle velocity at $\underline{r} = 0$, while Equation 16c is used to calculate the particle velocity at $\underline{r} = \underline{r}_{max}$. Equations 16b and 16c are used to calculate this difference in velocity for Tubes 2 and 3, respectively. The results show that the lengths of the parabolas grow at a rate of 1.19, 1.00, and 0.83 cm/min for tubes 1, 2, and 3, respectively. These results, of course, are only valid for the first 180 seconds of the experiment, at which point the potential gradient decreases to a lower value. Equations 16a-c may subsequently be used to calculate the parabolic growth velocities of 0.89, 0.80, and 0.70 cm/min for Tubes 1, 2, and 3, respectively, for the final 100 seconds of the first traverse. Figure 5 shows the theoretical (solid lines) and experimental (open points) lengths of the parabolic particle profiles. Although there was some difficulty in measuring the lengths of the parabolas from the photographs because of the fuzziness of their tails, the agreement between experiment and theory is very good. It should be emphasized that the particle velocity near the channel wall is a sensitive function of the distance from the channel wall, so that small errors in $\underline{r}_{max}$ can lead to relatively large errors in the minimum particle velocity and the parabolic length as a function of time. The agreement between experiment and theory shown in Figure 5, therefore, may be taken as a confirmation of the validity of the theoretical approach and assumptions used in this analysis.

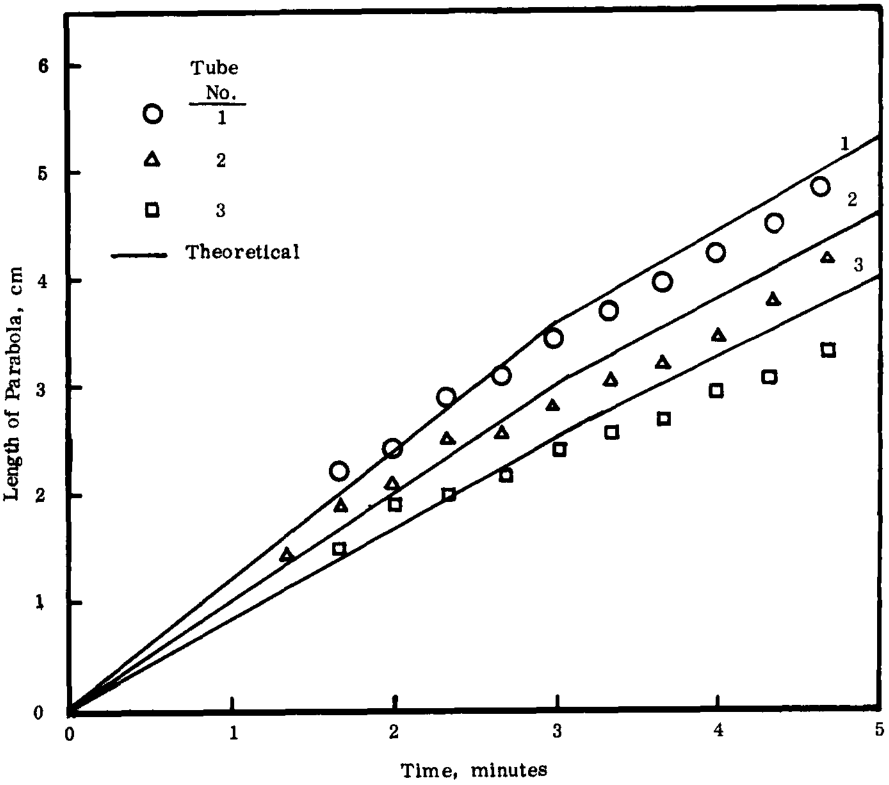

FIGURE 5

Variation of the Length of the Parabolic Particle Profiles with Time

The two different-size particles in Tube 1 actually separated, to form a parabolic cone of the slower-moving particles nested inside the parabolic cone of the faster-moving particles. Figure 6A shows the experimental results after 3 minutes and Figure 6B the corresponding calculated parabolic particle profiles. Figure 6C shows a black-and-white reproduction of the color contour densitometric scan (6) of the negative of Figure 6A. This method, which is more sensitive than conventional densitometry, produces a color photograph with different

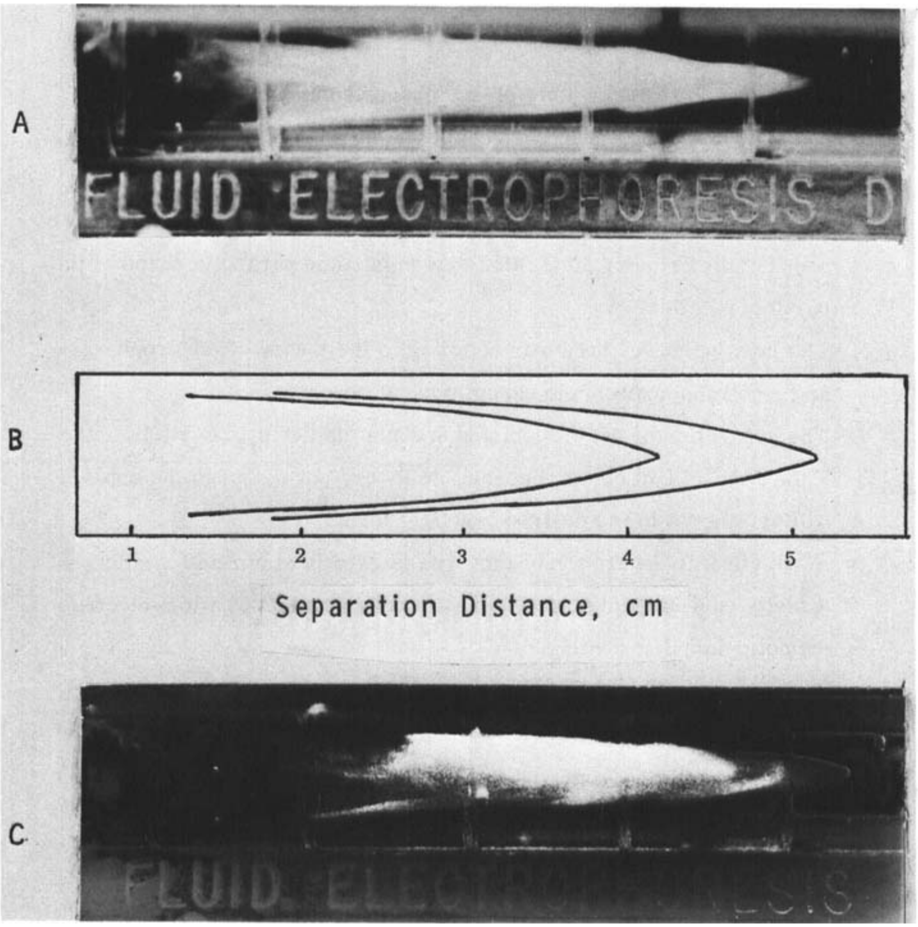

FIGURE 6

Free-fluid electrophoretic separation of mixed 0.80μm- and 0.23μm-diameter monodisperse polystyrene latex particles during Apollo 16 mission: A. photograph of separation after 3 minutes; B. theoretical prediction of separation shown in A.; C. black-and-white reproduction of color contour densitometric scan of photograph shown in A.

colors denoting areas of different density. The high-density area corresponding to the predicted overlap of the two parabolic cones confirms that separation of the different-size particles took place as predicted.

CONCLUSIONS

In the Apollo 16 free-fluid electrophoresis experiment:

1. The potential gradient in each channel was reduced by approximately 40% because of the presence of bubbles in the channels.
2. Electroosmosis was pronounced at the Lexan/buffer solution interface and was the primary factor that determined the parabolic shape of the particle profiles.
3. The latex particles behaved according to the theory of electrophoresis and electroosmosis in closed cylindrical channels.
4. The separation of the 0.80µm and 0.23µm diameter latex particles in Tube 1 did in fact occur according to theory, even though the separation was not in the desired practical form.
5. A practicable separation of this type is greatly simplified in microgravity environment, but requires the development of a low-electroosmotic-mobility coating.

ACKNOWLEDGMENT

Two of us (FJM and JWV) gratefully acknowledge support for this work by the National Aeronautics and Space Administration under contract No. NAS8-28654.

REFERENCES

1. H. A. Abramson, Electrokinetic Phenomena, The Chemical Catalog Co., Inc., New York, 1934, Chap. 1.
2. E. C. McKannan, A. C. Krupnick, R. N. Griffin, and L. R. McCreight, Electrophoresis Separation in Space - Apollo 14, NASA Technical Memorandum TMX-64611, 1971.

3. R. S. Snyder, M. Bier, R. N. Griffin, A. J. Johnson, H. L. Leidheiser, F. J. Micale, J. W. Vanderhoff, S. Ross, and C. J. van Oss, Separation and Purification Methods, 2(2), 259-282, 1973.
4. Supplied by The Dow Chemical Company, Midland, Michigan.
5. R. S. Snyder, Electrophoresis Demonstration on Apollo 16, NASA Technical Memorandum TMX-64724, 1972.
6. Private communication, N. Lamar, Johnson Space Center, Houston.